

## Research Article

# Computer-Aided Diagnosis of Muscle Mass through Antenna as a Sensor

Sesha Vidhya S. <sup>1</sup>, Rukmani Devi <sup>2</sup> and Shanthi K. G.<sup>1</sup>

<sup>1</sup>Department of Electronics and Communication Engineering, RMK College of Engineering and Technology, Tamil Nadu, India

<sup>2</sup>Department of Electronics and Communication Engineering, RMD Engineering College, Tamil Nadu, India

Correspondence should be addressed to Sesha Vidhya S.; [sesha12345rmk@gmail.com](mailto:sesha12345rmk@gmail.com)

Received 7 September 2022; Revised 22 November 2022; Accepted 24 November 2022; Published 22 December 2022

Academic Editor: Antonio Lazaro

Copyright © 2022 Sesha Vidhya S. et al. This is an open access article distributed under the Creative Commons Attribution License, which permits unrestricted use, distribution, and reproduction in any medium, provided the original work is properly cited.

Wireless body area network (WBAN) incorporates a wireless sensor network and wearable devices in miniature size. In this paper, a dual-band microstrip patch (DBMSP) antenna as a sensor with a modified split ring resonator (SRR) and defective ground structure (DGS) is proposed for muscle mass measurement and prediction. Modified SRR on the ground plane forms a defected ground structure (DGS) for back radiation reduction and suits muscle mass measurement. The proposed dual-band microstrip patch antenna resonates at 5.2 GHz and 8.4 GHz, with impedance bandwidth of about 0.9 GHz and 1.89 GHz, input reflection coefficient is about -21.12 dB and -14.5 dB, respectively. This DBMSP antenna has an efficiency of 99.9%, with a negligible amount of specific absorption rate (SAR). From the proposed DBMSP antenna sensor, muscle mass is predicted from human muscle. The proposed antenna is fixed on the ventral surface of the forearm and biceps. DBMSP antenna sensor detects electromagnetic energy from muscle tissues under radiating near-field conditions. The muscle tissue signal is acquired through the proposed DBMSP antenna. The acquired antenna process with nondecimated wavelet transform (NDWT) and discrete wavelet transform (DWT) algorithms for noise reduction. Further, early prediction of muscle mass prevents humans from lack of protein and oxygen levels in the blood and avoids major issues in human health. The proposed DBMSP antenna-based muscle mass measurement achieves 89% accuracy when compared with laboratory measurement.

## 1. Introduction

Wireless body area network (WBAN) has widened due to the growth in wireless sensor networks and low-power devices. Low-power controllers and devices lead to portability, flexibility, and mobility in wearable devices. WBAN is used for instance remote patient monitoring, biofeedback, smartwatches, and bags for health monitoring [1–3]. WBAN is used for different health monitoring on daily basis, such as heart rate, temperature, blood pressure, electrocardiogram (ECG) signals, etc., and nonmedical applications [4, 5]. In WBAN, antennas are low cost, lightweight, and maintenance free. Wearable antenna design should be of low radiation efficiency. Moreover, body-centric wireless communication systems (BWCS) are classified as on body, off body, and in-body/implanted communications [6–8]. End-fire planar

Yagi-Uda's antenna with AMC as a back reflector provides higher efficiency and low SAR with better impedance matching [9]. Circularly polarized antennas made of polydimethylsiloxane (PDMS) and silver nanowire (AgNW) are analyzed in the human body for structural deformation conditions [10]. A planar broadband antenna is integrated with an artificial magnetic conductor and provides low backward radiation smaller in size, with low SAR, high front-to-back ratio, and high gain, which are suitable for wireless body area applications [11]. A compact double circular ring, wider bandwidth and smaller size antenna, is designed for UWB biomedical application [12, 13]. Circularly polarized implantable antenna loaded with complementary split ring resonators (CSRR) for real-time glucose monitoring is presented and provides high gain, wide beam width, and low SAR [14]. Metasurface-based antenna improves the radiation characteristics and

energy absorption from the human tissue. Furthermore, low SAR and high front-to-back ratio are suitable for body area wearable applications [15].

Muscle mass is about the muscles in human body, which consists of skeletal muscles, smooth muscles, and cardiac muscles. Muscle mass is measured as a part with other mass such as fat and bone mass. Skeletal muscle is about muscle fibers. Single muscle cell is bounded and wrapped with connective tissues and termed as epimysium. Approximately, 20 to 80 muscle fibers together form as fascicle. Human muscles are differentiated by the connective tissues outside the epimysium, and termed as fascia. Tendons join the muscles to the human bone. Body mass has various components such as body fat and lean body mass. Muscle mass plays a vital role for different human activities such as mobility, balance, and strength. Muscle mass measurement in human body is difficult due to different factors such as height, ethnicity, and fitness. Novel method is required for the human muscle mass of persons at different age groups. Muscle mass reduction is caused due to increase in degradation and decrease in synthesis of the human muscle proteins. The outcome of muscle mass reduction leads to change in the structure of muscle fibers [16–21].

Muscle mass is diagnosed using heterogeneous diagnostic criteria. Muscle mass is assessed either/both quantitatively and qualitatively. Earlier detection of skeletal muscle mass measurement prevents metabolic side effects such as diabetes, depression, abnormal cholesterol levels, and weight gain. The major disadvantage of existing muscle mass measurement method is the long exposure of radiation on the human body. In DXA-based muscle mass measurement, radiation dose changes over the different locations of the human muscle region and leads to inaccurate measurement. Measurements of skeletal muscle mass using body fat percentages are approximate and unreliable. The precise muscle mass measurement never determined through human body diameter and composition. However, lean mass is assessed based on the height of a person and not qualitatively from the human muscle. In this paper, noninvasive technique for predicting muscle mass is performed through the passive flexible UWB-myogram antenna sensor signals. Myogram antenna acquires muscle dielectric radiation from various muscle locations of human body.

- (i) To develop passive flexible dual-band microstrip patch (DBMSP) antenna as sensor and fixed the antenna on the muscle surface of human body for acquiring the dielectric radiation from muscle for muscle mass measurement
- (ii) To denoise the signals from antenna through DWT and NDWT algorithms for measurement of human muscle mass
- (iii) The structural alternation in any skeletal muscle surface leads to change in the dielectric property of muscle at that particular location; changes are seen in the antenna acquired muscle radiation signal. Linear regression is modelled and proposed for the human muscle mass measurement

## 2. Literature Survey

Different types of antenna are used as sensor in biomedical applications. Microstrip patch antenna is widely used in wireless applications due to low profile, low cost, reduced fabrication complexity, and lightweight and simple architecture [22, 23]. Microstrip antenna has unidirectional radiation pattern and low specific absorption rate (SAR), which is required for biomedical applications. Microstrip antennas have very narrow bandwidth, which is a function of the dielectric constant of substrate and substrate thickness. This leads to focus on substrate selection during the process of antenna design [24, 25]. Dual band textile antenna based on artificial magnetic conductor (AMC) is tested for specific absorption rate (SAR). From testing, AMC structured antenna has SAR, whereas the size of the antenna is big i.e., (120 mm × 120 mm) [26, 27]. A compact monopole antenna made with Kapton polyimide as substrate with a dielectric constant of 3.5 and loss tangent of slotted AMC ground plane is about 0.002 and designed for telemedicine applications with an operating frequency of 2.45 GHz. The SAR value is low of about 64%, when compared to the similar shape of antennas without AMC. From the analysis, return loss and shift in resonant frequency are low [28–30]. A wearable antenna operating at 700 MHz is designed with polycarbonate substrate and with AMC as 2\*2 arrays at the base and has return loss ( $S_{11}$ ) of about -25 dB, gain of about 3.7 dBi, efficiency of about 50%, and the size antenna is big i.e., (60 mm\*60 mm) [31, 32]. A folded dipole antenna with AMC as a ground plane has the low SAR and impedance mismatching due to the nearness of human body tissues are reduced [33, 34]. The performance metrics of a square shaped SRR antenna are compared with a square shaped closed ring resonator (CRR) microstrip antenna. The squared SRR antenna has a gain of about 8.9 dB, efficiency of about 97.75%, and SAR of about 0.163 W/Kg. SRR antenna outperforms the CRR antenna [35]. A miniaturized UWB slot antenna with tuneable frequency, reconfigurable structure based on S-shaped split ring resonators (S-SRRs), is designed using CSRR [36–38].

Smaller size antenna is the foremost requirement in biomedical applications. The problems due to reduction patch size in antenna degrade the efficiency, bandwidth, gain, and swing in resonant frequency. Henceforth, researchers focus on small size antenna and with better performance for biomedical application. In this paper, circular shape double ring patch antenna is designed with a square-shaped double split ring resonator (SRR) with defective ground structure (DGS) loaded on the ground surface and operates at the frequency of 5.2 GHz. The proposed patch antenna is smaller in size, and Arlon is used as the substrate material, which has a relative permittivity of 10.2. The main objective of this proposed antenna design is high gain and directivity, which in turn increases the radiation efficiency of the antenna and minimizes the size.

## 3. Design and Structure of DBMSP Antenna

The proposed DBMSP antenna sensor consists of dual band antenna geometry. The DBMSP antenna consists of two

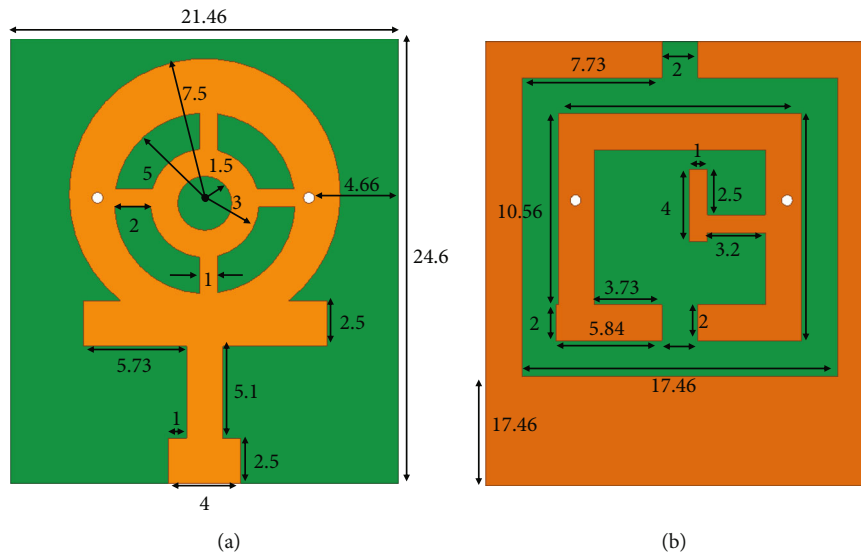


FIGURE 1: DBMSP antenna sensor geometry. (a) Top view. (b) Bottom view.

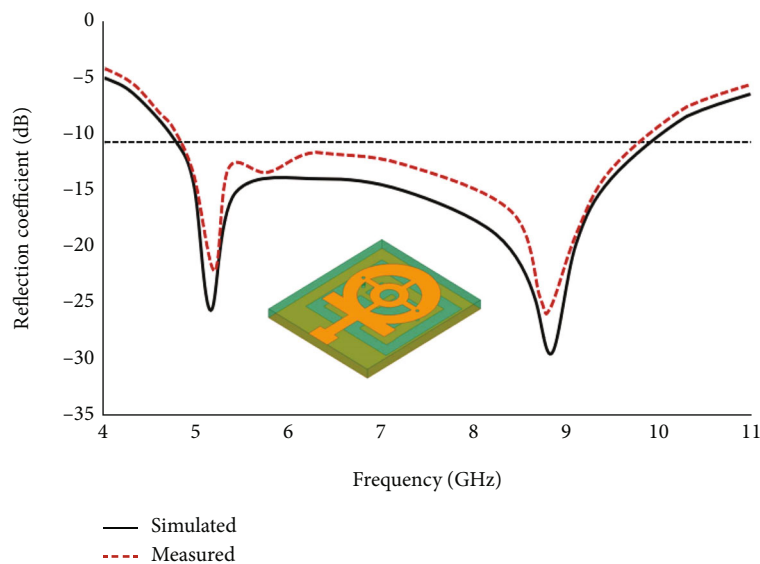


FIGURE 2: Simulated and measured reflection coefficient in dB of DBMSP antenna sensor.

hollow rings with four strips (i.e., wheel shape) connected to a T-shaped feed and has a modified SRR-shaped ground plane as shown in Figure 1. DBMSP antenna sensor geometry shown in Figures 1(a) and 1(b), respectively. The size of the substrate is about  $21.46 \times 24.6 \times 1.6$ . In Figure 1(a), microstrip line feed is connected to the edge of the radiating patch and leads to impedance mismatch and solved through stubs. Stubs are widely used for reducing impedance mismatch. It is positioned at a distance, so the real part of admittance is in unity. The length of the stub is 7.6 mm, and the width of the stub is 4 mm. A closed ring resonator is on the patch, which acts as radiator. To increase the performance of the proposed DBMSP antenna sensor, inductance slots are integrated into the patch. The radius of the patch is  $r_1 = 7.5$  mm and  $r_2 = 3$  mm, and the width of the inductance slot is

1 mm. Furthermore, air holes are drilled on the antenna, avoids the spurious radiations, when antenna is close to the human body, and achieves circular polarization. Arlon is used as the substrate material because of its high dielectric radiation absorption and helps in reducing the size, low insertion loss, inexpensive, light in weight, and offers robustness. Therefore, Arlon material suits for low impedance. The radiation from the antenna is in positive and negative  $z$ -axis.

Metamaterial is used at the bottom of the substrate and reduces the back radiations. It provides protection to the underlying tissues. Metamaterial observes the human body muscle dielectric material radiation. Metamaterial has extraordinary properties such as negative permittivity, permeability, and refractive index. Metamaterial is composed of a metallic wire array and split ring resonator. Split ring

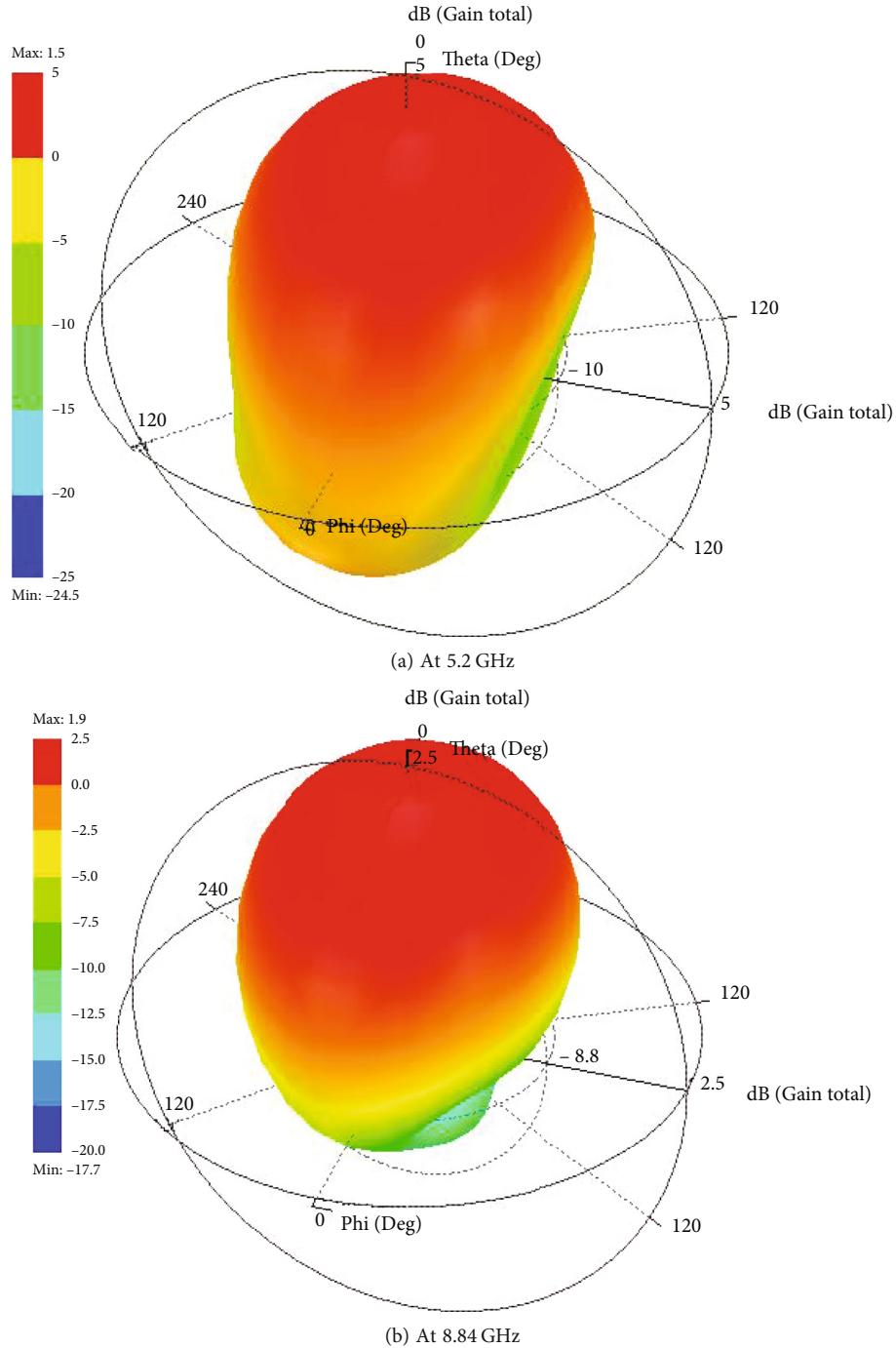


FIGURE 3: Radiation pattern of DBMSP antenna sensor.

resonator is a LC circuit. When dielectric radiation from human muscles is perpendicular to the split ring resonator, current will be induced in the DBMSP antenna. Due to the splits in the circuit, current flow charges developed in the gap and the energy will be stored in capacitance. For frequencies below the resonant frequency, split ring resonator keeps the magnetic field and provides a positive response. As the frequency increases, SRR never keeps the H field; thereby, negative response is produced. Figure 2 shows the frequency bandwidth range and reflection coefficient of sim-

ulated DBMSP antenna and compared with measured values from fabricated antenna, closely matches with simulated and fabricated result. A reflection coefficient of below -24 dB indicates the 1% of reflection and 99% of power.

Due to the modified SRR structure with holes and DGS at the ground plane of antenna, the lower back radiation is observed and shown in Figure 3.

Figure 4 shows the current distribution at two different resonant frequencies. From the results, it is observed that the concentration of current is high at the feed and circular ring region.

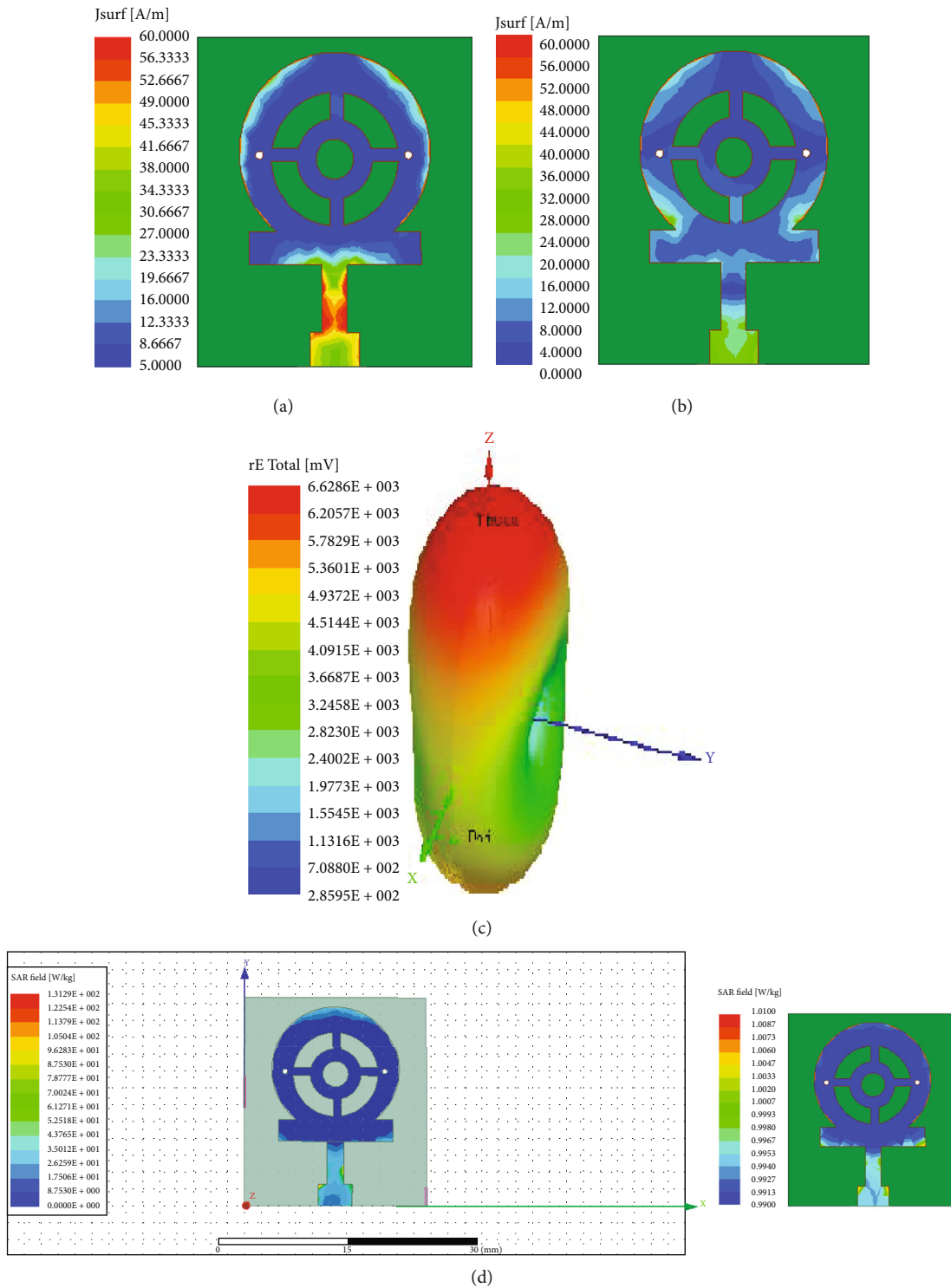


FIGURE 4: DBMSP antenna sensor current distribution at (a) 5.2 GHz, (b) 8.4 GHz, (c) gain plot, and (d) SAR.

Figure 5 shows the block diagram of DBMSP antenna sensor to diagnose muscle mass from ventral surface of forearm. The relationship between Gain and Efficiency is  $G = \text{efficiency} \times \text{directivity}$ . Since gain and directivity has similar values, the efficiency is improved of about 99.9%, and  $\text{efficiency} = G/D$ . SAR value of the MIMO smartphone on human tissue is evaluated at different frequencies such

as 3.5 GHz and 5.1 GHz [30]. To overcome the high SAR value, a modified split ring resonator with DGS is included at the base of the DBMSP for muscle mass predication. This DGS avoids spurious radiations and increases the performance of the antenna. The DBMSP antenna simulation is done using high frequency structure simulator (HFSS) software. Figure 5 shows the protein measurement



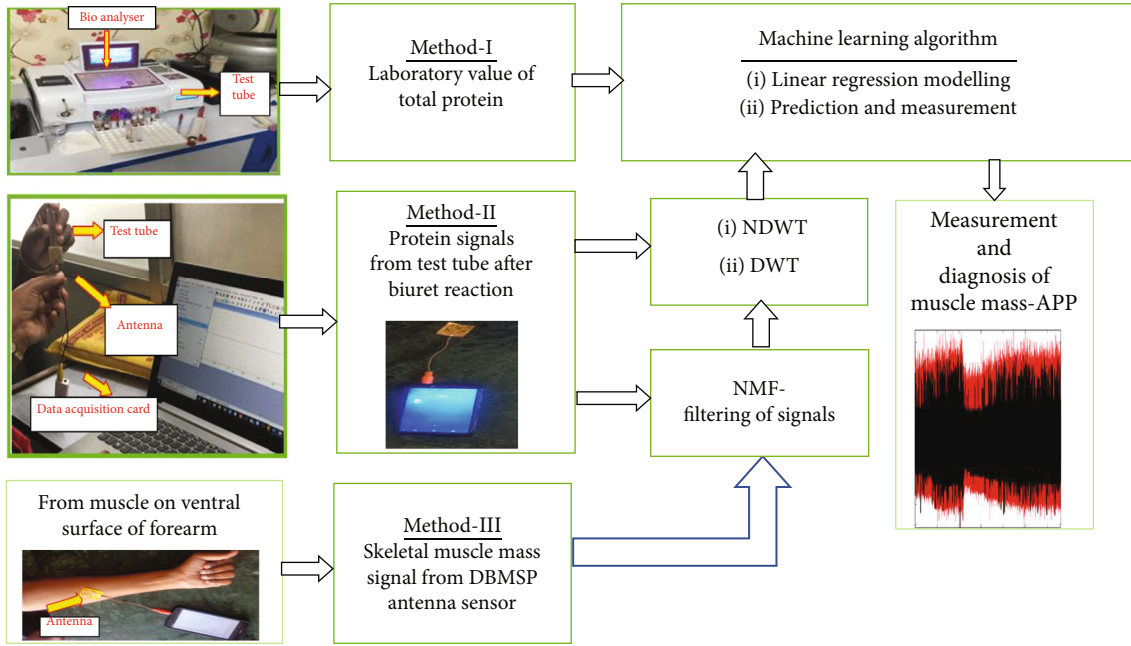


FIGURE 5: Passive DBMSP antenna sensor to diagnose muscle mass from ventral surface of forearm.

and correlated with laboratory values and diagnosed the muscle mass disease.

In method I, protein in the human blood is measured from blood sample in the test tube and added protein dissolvent in the test tube for biuret reaction, measured the protein value through analysers. In method II, the proposed DBMSP antenna is placed over the test tube, which contains the violet “biuret” complex protein and acquired the dielectric radiations of protein. The DBMSP acquired signals are save in computer using data acquisition toolbox of MATLAB software. In method III, the proposed DBMSP antenna sensor is fixed on the ventral surface of forearm muscle and measured the protein in the muscle through DBMSP acquired signals. The acquired signals are saved using MATLAB. DBMSP acquired signals from method II (test tube) and method III (human forearm muscle) are filtered using blind source separation such as nonnegative matrix factorization (NMF) method. The filtered signals are then processed with DWT and NDWT. Then, statistical values from DWT and NDWT processed signals are correlated with the machine learning algorithm such as linear regression for prediction of muscle mass.

**3.1. Discrete Wavelet Transform (DWT).** The discrete wavelet transform (DWT) divides a signal into many sets. DWT transform is used to denoise the real signal. DWT breaks down an original signal, eliminates noise, and decomposes the signal.

$$\varphi(x) = \sum_{k=-\infty}^{\infty} (-1)^k a_{N-1-k} \varphi(2x - k), \quad (1)$$

where  $N$  is an even integer,  $a$  and  $k$  define scaling functions, and  $\Psi$  is a wave function. DWT algorithm detects the

fine structure in the signal. In muscle mass monitoring, DWT method is used to analyse the muscle mass signals. DWT is noninvariant, sensitive to signal time alignment.

**3.2. NDWT.** NDWT is a type of wavelet transform that addresses the shortcomings of DWT. In NDWT decomposition, signals are divided into many frequency bands. After removing the downsamplers from NDWT, there is no lack of translation invariance. The fundamental disadvantage of DWT is translation invariance. NDWT is a redundant method, which has same level of output samples as the input. Signal denoising, pattern identification, brain picture/classification, and diseased brain detection are few applications for NDWT. Denoising is the primary goal of NDWT.


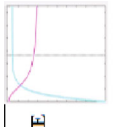
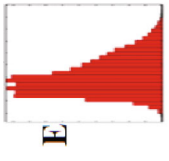
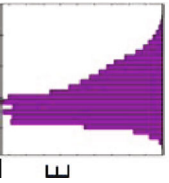
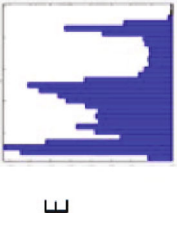
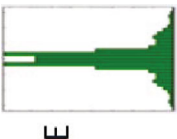
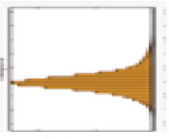

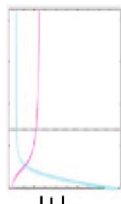
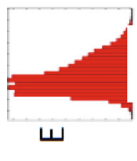
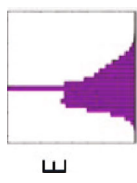
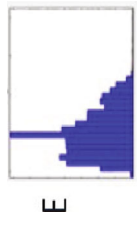
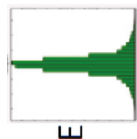
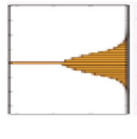
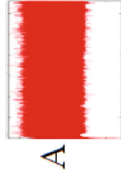
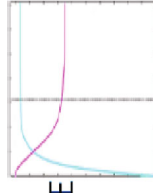
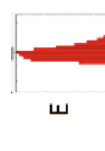
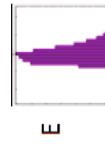

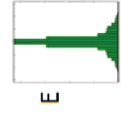
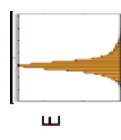
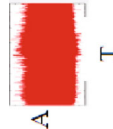
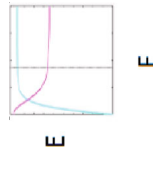
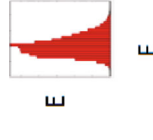
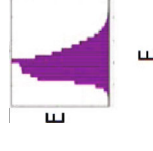
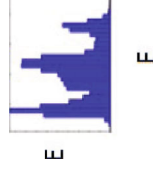
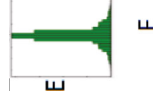
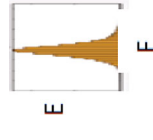

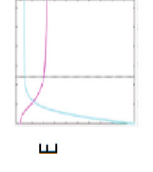
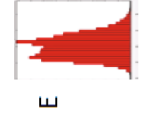
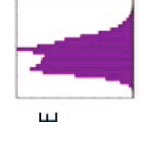
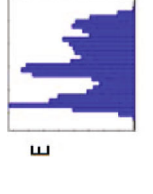

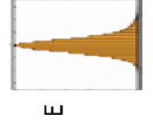
## 4. Results and Discussion

The proposed DBMSP antenna design is with modified SRR and DGS, simulated using HFSS, and the performance of the antenna signal is analysed with histogram. Table 1 shows the output of DWT algorithm.

Table 1 shows the histogram outputs such as original histogram, synthesized histogram, approximation histogram, details histogram, and compressed signal with signals of five different patients (male) at different ages such as 17 of age, 21 of age, 33 of age, 35 of age, and 38 of age. Figure 6 shows the output of denoised signals for DWT and NDWT.

Figure 6 shows the denoised signal of different aged persons after processed with DWT and NDWT algorithms. NDWT has noise compared to DWT algorithm. The mean value of DBMSP antenna sensor signal is obtained after processing with NDWT method and used for muscle mass measurement with linear regression. Table 2 shows comparison of signals based on statistical parameters for 17 to 38 aged patients.

TABLE 1: DWT processed DBMSP antenna sensor signals.

Input signal and patient age for DWT	Compressed muscle mass signal	Original histogram of muscle mass signal	Synthesized histogram of muscle mass signal	Approximation histogram of muscle mass signal	Details histogram of muscle mass signal	Residual histogram
 17 age male	 E F	 E F	 E F	 E F	 E F	 E F
 21 age male	 E F	 E F	 E F	 E F	 E F	 E F
 33 age male	 E F	 E F	 E F	 E F	 E F	 E F
 35 age male	 E F	 E F	 E F	 E F	 E F	 E F
 38 age male	 E F	 E F	 E F	 E F	 E F	 E F

\*A: amplitude; T: time; E: energy; F: frequency.

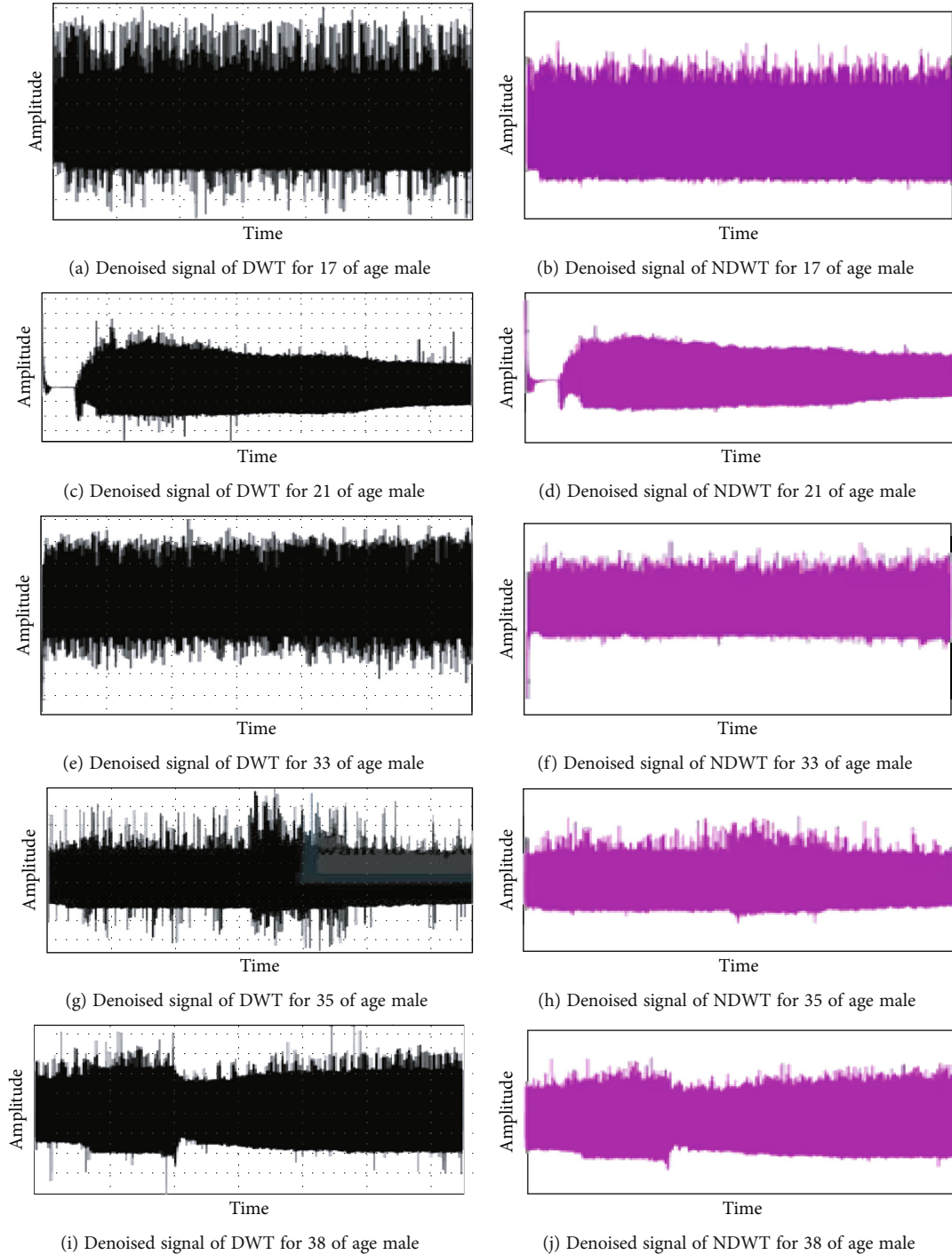


FIGURE 6: Denoised output of DWT and NDWT algorithms DBMSP antenna sensor signals.

Table 2 shows the average values of peak amplitude, mean, and standard deviation of people with different gender and persons with age between 17 and 38 years. Table 1 displays the male protein levels with respect to the protein measurement from medical laboratory. The mean value of signal is high due to muscle thickness and wider distribution of tissues in young age. The same is validated through maximum radiation of the signals acquired by proposed DBMSP antenna sensor from muscles, and the corresponding voltage

signals show the increase. From Table 2, the inference is that the person with low protein has highest peak amplitude and mean value after processing with NDWT, whereas the person with high protein has lowest peak amplitude and low mean value. Figure 7 shows the output of linear regression.

In Figure 7(a), linear regression is plotted between mean value of DBMSP antenna sensor signal processed with NDWT and medical laboratory value of protein. Figure 7(b) shows the residual plot. Linear regression gives



TABLE 2: Comparison of DBMSP antenna sensor signals and parameters for 17 to 38 years patients.

Patient age male/female	Antenna location for acquiring signal	Signal (mV)	Mean	SD	Laboratory protein value (g/dL)
17 years	Test tube	145	189	16.2	8.5 (medium)
	Bicep-long heads	143	96	15.4	
	Ventral surface of forearm	132	89	16.5	
21 years	Test tube	173	274	16.1	8.6
	Bicep-long heads	145	89	14.6	
	Ventral surface of forearm	150	98	15.3	
33 years	Test tube	150	96	15.5	8.4 (low)
	Bicep-long heads	142	100	14.7	
	Ventral surface of forearm	137	104	13.9	
35 years	Test tube	150	178	15.6	8.7
	Bicep-long heads	132	87	16.5	
	Ventral surface of forearm	164	96	14.3	
38 years	Test tube	140	167	14.6	8.8 (high)
	Bicep-long heads	139	81	13.3	
	Ventral surface of forearm	129	89	15.6	

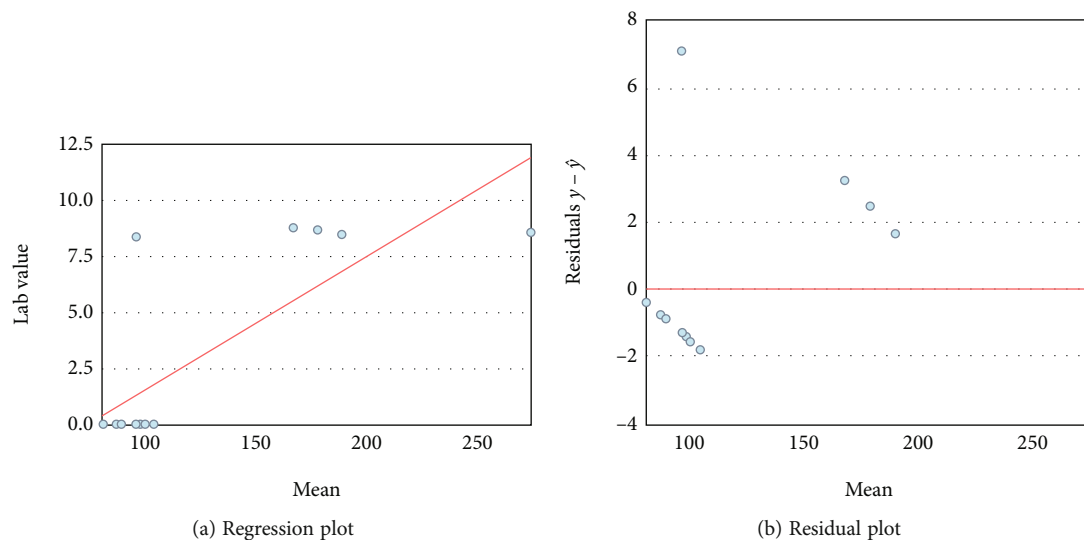


FIGURE 7: Linear regression of proposed DBMSP antenna signal.

TABLE 3: Comparison of DBMSP antenna sensor and traditional method.

Method	Reproducibility	Time of measurement	Radiation (m rem)	Cost
DXA [32]	3%	10-20 min.	0.5	High
BIA [33]	3% (62)	1 min.	0	Low
CT [35]	<2%	10 sec.	200	High
MRI [34]	3%	1-10 min.	0	High
Proposed algorithm (DBMSP)	<1%	<1 min.	0.1	Very high

high accuracy compared to other methods. The accuracy calculated from regression.

$$\text{Lab value of muscle mass} = 0.0598 * \text{mean} - 4.444. \quad (2)$$

The regression analysis predicts and investigates the relationship between a dependent (laboratory protein value) and

independent variable such as mean value of skeletal muscle from biceps or ventral surface. Regression modeling technique is applied for forecasting, time series modelling, and finding the causal effect relationship between the variables. Here, laboratory protein value and mean value of skeletal muscle from biceps or ventral surface were used for muscle mass predictions. Linear regression establishes a relationship

based on best-fit regression line. This linear equation gives  $R$ -squared value of 0.857. The average of the  $R$ -squared value proves muscle mass measurement has high performance. Table 3 shows comparison of proposed method with traditional methods.

## 5. Conclusion

This paper presents a DBMSP antenna sensor with modified SRR and DGS structure for human muscle mass prediction. The performance of the proposed DBMSP antenna sensor configuration is analysed and compared with various antenna configurations for muscle mass prediction. The proposed DBMSP antenna sensor signal processed with NDWT shows better accuracy in prediction of muscle mass. The comparison of performance metrics elucidates that the designed antenna outperforms all other configurations and yields higher gain, efficiency of about 99% and SAR of about 0.001 W/Kg. The results clearly communicate that the proposed DBMSP antenna sensor with modified SRR and DGS is suitable for muscle mass prediction. From the prediction equation, a protein value of less than eight represents the normal muscle mass, and below seven indicates abnormal condition. The proposed method of muscle mass disease identification is applied for 17 to 38 of age group people and compared with their medical laboratory values. The proposed DBMSP antenna sensor-based muscle mass prediction has accuracy of 89%, when compared to muscle mass prediction through protein value from laboratory method. Moreover, the DBMSP antenna sensor-based muscle mass prediction avoids the picking of blood from person for muscle mass measurement. Moreover, region wise muscle mass measurement i.e., each part can be done through proposed DBMSP antenna sensor-based method. Furthermore, the proposed DBMSP antenna sensor-based muscle mass prediction can be applied for the senior citizens.

## Data Availability

The datasets generated during the current study are available from the corresponding author on reasonable request.

## Disclosure

The presentation of the manuscript was in Research Square and also included in the reference.

## Conflicts of Interest

The authors declare that they have no conflicts of interest to report regarding the present study.

## References

- [1] Y. S. Chen and T. Y. Ku, "A low-profile wearable antenna using a miniature high impedance surface for smartwatch applications," *IEEE Antennas Wireless Propagation Letters*, vol. 15, no. 4, pp. 1144–1147, 2016.
- [2] G. Monti, L. Corchia, E. D. Benedetto, and L. Tarricone, "Wearable logo-antenna for GPS–GSM-based tracking systems," *IET Microwave Antennas Propagation*, vol. 10, no. 12, pp. 1332–1338, 2016.
- [3] L. Vallozzi, P. V. Torre, C. Hertleer, H. Rogier, M. Moeneclaey, and J. Verhaevert, "Wireless communication for firefighters using dual-polarized textile antennas integrated in their garment," *IEEE Trans. Antennas Propagation*, vol. 58, no. 4, pp. 1357–1368, 2010.
- [4] S. Movassaghi, M. Abolhasan, J. Lipman, D. Smith, and A. Jamalipour, "Wireless body area networks: a survey," *IEEE Communication*, vol. 16, no. 3, pp. 1658–1686, 2014.
- [5] M. Patel and J. Wang, "Applications, challenges, and prospective in emerging body area networking technologies," *IEEE Trans. Wireless Communication*, vol. 17, no. 1, pp. 80–88, 2010.
- [6] C. Liu, Y.-X. Guo, and S. Xiao, "A review of implantable antennas for wireless biomedical devices. Forum for electromagnetic research methods and application technologies," *Microprocessors and Microsystems*, vol. 79, no. 43, article 103284, 2016.
- [7] P. S. Hall and Y. Hao, "Antennas and propagation for body-centric wireless communications. MA: Artech house," *IEEE Antennas and Propagation Magazine*, vol. 55, no. 5, pp. 97–117, 2013.
- [8] S. Sessa Vidhya, S. Rukmani Devi, and K. G. Shanthi, "Design trends in ultra wide band wearable antennas for wireless on-body networks," *ARNP Journal of Engineering and Applied Sciences*, vol. 12, no. 9, pp. 1819–6608, 2017.
- [9] K. Agarwal, Y.-X. Guo, and B. Salam, "Wearable AMC backed near-end fire antenna for on-body communications on latex substrate," *IEEE Transactions on Components, Packaging and Manufacturing Technology*, vol. 6, no. 3, pp. 346–358, 2016.
- [10] Z. H. Jiang, Z. Cui, T. Yue, Y. Zhu, and D. H. Werner, "Compact, highly efficient, and fully flexible circularly polarized antenna enabled by silver nanowires for wireless body-area networks," *IEEE Transactions on Biomedical Circuits and Systems*, vol. 11, no. 4, pp. 920–932, 2017.
- [11] X. Liu, Y. Di, H. Liu, Z. Wu, and M. M. Tentzeris, "A planar windmill-like broadband antenna equipped with artificial magnetic conductor for off-body communications," *IEEE Antennas and Wireless Propagation Letters*, vol. 24, no. 2, pp. 2429–2683, 2017.
- [12] Z. Khan, A. Razzaq, J. Iqbal, A. Qamar, and M. Zubair, "Double circular ring compact antenna for ultra-wideband applications," *IET Microwaves Antennas Propagation*, vol. 45, no. 21, pp. 2094–2097, 2018.
- [13] S. Sessa Vidhya, D. Rukmani Devi, K. G. Shanthi, and S. Venkatesan, "Performance enhancement of micro strip UWB patch antenna with SRR for wireless body area networks," *Int. J. Innov. Technol. Explor. Eng. (IJITEE)*, vol. 52, no. 22, pp. 112–115, 2019.
- [14] X. Y. Liu, W. ZeTao, Y. Fan, and M. M. Tentzeris, "A miniaturized CSRR loaded wide-beamwidth circularly polarized implantable antenna for subcutaneous real-time glucose monitoring," *IEEE Antennas and Wireless Propagation Letters*, vol. 53, no. 21, pp. 577–580, 2016.
- [15] M. Guangchen and P. Ren, "A compact dual-band metasurface-based antenna for wearable medical body-area network devices," *Journal of Electrical and Computer Engineering*, vol. 2020, no. 2, Article ID 4967198, p. 10, 2020.
- [16] W. J. Evans, "Skeletal muscle loss: cachexia, sarcopenia, and inactivity," *The American Journal of Clinical Nutrition*, vol. 91, no. 4, pp. 1123S–1127S, 2010.

- [17] S. Sessa Vidhya, S. Rukmani Devi, and K. G. Shanthi, "Human muscle mass measurement through passive flexible UWB-myogram antenna sensor to diagnose sarcopenia," *Microprocessors and Microsystems*, vol. 79, article 103284, 2020.
- [18] C. V. Albanese, E. Diessel, and H. K. Genant, "Clinical applications of body composition measurements using DXA," *Journal of Clinical Densitometry*, vol. 6, pp. 75–85, 2003.
- [19] L. R. A. de Lima, C. R. Rech, and E. L. Petroski, "Use of bioelectrical impedance for the estimation of skeletal muscle mass in elderly men," *Archivos Latinoamericanos de Nutrición*, vol. 58, no. 4, pp. 386–391, 2008.
- [20] J. A. Houmard, R. Smith, and G. L. Jendrasiak, "Relationship between MRI relaxation time and muscle fiber composition," *Journal of Applied Physiology*, vol. 78, no. 3, pp. 807–809, 1995.
- [21] K. Imamura, H. Ashida, T. Ishikawa, and M. Fujii, "Human major psoas muscle and sacrospinalis muscle in relation to age: a study by computed tomography," *Journal of Gerontology*, vol. 38, no. 6, pp. 678–681, 1983.
- [22] H. I. Hraga, C. H. See, R. A. Abd-Alhameed, and N. J. Mcewan, "Miniaturized UWB antenna for a wireless body area network," *Loughborough, UK*, vol. 53, no. 31, 2012.
- [23] J. C. Wang, E. G. Lin, M. Leach, Z. Wang, K. L. Man, and Y. Huang, *Conformal Wearable Antennas for WBAN Application*, vol. 23, no. 12, 2016, IMECS, Hongkong, 2016.
- [24] L. Liu, S. Zhu, and R. Langley, "Dual-band triangular patch antenna with modified ground plane," *Electronics Letter*, vol. 43, no. 3, pp. 140–141, 2007.
- [25] C. T. Islam, M. Faruque, and N. Misran, "Reduction of specific absorption rate (SAR) in the human head with ferrite material and metamaterial," *Progress In Electromagnetics Research C*, vol. 9, no. 12, p. 4758, 2009.
- [26] S. Zhu and R. Langley, "Dual-band wearable textile antenna on an EBG substrate," *IEEE Trans. on Antennas and Propagation*, vol. 57, no. 4, pp. 926–935, 2009.
- [27] H. R. Raad, A. I. Abbosh, H. M. Al-Rizzo, and D. G. Rucker, "Flexible and compact AMC based antenna for telemedicine applications," *IEEE Transactions on Antennas and Propagation*, vol. 61, no. 2, pp. 524–531, 2013.
- [28] S. Genovesi, F. Costa, F. Fanciulli, and A. Monorchio, "Wearable inkjet-printed wideband antenna by using miniaturized AMC for sub-GHz applications," *IEEE Antennas Wireless Propagation Letters*, vol. 15, no. 12, pp. 1927–1930, 2016.
- [29] S. Yan, P. J. Soh, and G. A. E. Vandenbosch, "Low-profile dual-band textile antenna with artificial magnetic conductor plane," *IEEE Transactions on Antennas and Propagation*, vol. 62, no. 12, pp. 123–132, 2014.
- [30] J. VallecchiDe, F. C. Luis, and F. De Flaviis, "Low profile fully planar folded dipole antenna on a high impedance surface," *IEEE Trans. on Antennas and Propagation*, vol. 60, no. 1, pp. 51–62, 2012.
- [31] S. Sessa Vidhya, S. Rukmani Devi, K. G. Shanthi, and N. Nowshith Parveen, "Design of UWB slot antenna for WBAN application," *International Journal of Current Research and Review (IJCR)*, vol. 13, no. 6, pp. 150–154, 2021.
- [32] K. Horestani, Z. Shaterian, J. Naqui, F. Martin, and C. Fumeaux, "Reconfigurable and tunable S-shaped split ring resonators and application in band-notched UWB antennas," *IEEE Transactions on Antennas and Propagation*, vol. 23, no. 12, pp. 3766–3776, 2017.
- [33] T. Yue, Z. H. Jiang, A. H. Panaretos, and D. H. Werner, "A compact dual-band antenna enabled by a complementary split ring resonator loaded metasurface," *IEEE Transactions on Antennas and Propagation*, vol. 56, no. 23, pp. 2758–2821, 2017.
- [34] J. Kulkarni, A. G. Alharbi, A. Desai, C. Y. D. Sim, A. Poddar, and A. Desai, "Design and analysis of wideband flexible self-isolating MIMO antennas for sub-6 GHz 5G and WLAN smartphone terminals," *Electronics*, vol. 10, no. 23, p. 3031, 2021.
- [35] T. S. Bird, "Definition and misuse of return loss [report of the transactions editor-in-chief]," *IEEE Antennas and Propagation Magazine*, vol. 51, no. 2, pp. 166–167, 2009.
- [36] R. Li, C. Wu, X. Sun, Y. Zhao, and W. Luo, "An EBG-based triple-band wearable antenna for WBAN applications," *Micro-machines*, vol. 13, no. 11, p. 1938, 2022.
- [37] P. Kumar, T. Ali, and A. Sharma, "Flexible substrate based printed wearable antennas for wireless body area networks medical applications (review)," *Radio electronics and Communications Systems*, vol. 64, no. 7, pp. 337–350, 2021.
- [38] D. M. John, S. Vincent, S. Pathan, P. Kumar, and T. Ali, "Flexible antennas for a Sub-6 GHz 5G band: a comprehensive review," *Sensors*, vol. 22, no. 19, p. 7615, 2022.